HHS Public Access

Author manuscript

Microfluid Nanofluidics. Author manuscript; available in PMC 2019 September 24.

Published in final edited form as:

Microfluid Nanofluidics. 2010 April ; 8(4): 457–465.

Cell motion and recovery in a two-stream microfluidic device

Clara Mata, **Ellen Longmire**

Aerospace Engineering and Mechanics, University of Minnesota, 110 Union Street SE, Minneapolis, MN 55455, USA

David McKenna

Clinical Cell Therapy Laboratory, University of Minnesota, 420 Delaware Street, Minneapolis, MN 55455, USA

Katie Glass, **Allison Hubel**

Department of Mechanical Engineering,University of Minnesota, 1100 Mechanical Engineering, 111 Church Street SE, Minneapolis, MN 55455, USA

Allison Hubel: hubel001@umn.edu

Abstract

The motion of cells in a two-stream microfluidic device designed to extract cryoprotective agents from cell suspensions was tested under a range of conditions. Jurkat cells (lymphoblasts) in a 10% dimethylsulfoxide solution were driven in parallel with phosphate-buffered saline solution wash streams through single rectangular channel sections and multiple sections in series. The influence of cell-stream flow rate and cell volume fraction (CVF) on cell viability and recovery were examined. The channel depth was 500 lm, and average cell stream velocity within the channels was varied from 3.6 to8.5 mm/s corresponding with cell stream Reynolds numbers of 2.6–6.0. Cell viability measured at device outlets was high for all cases examined indicating no significant cell damage within the device. Downstream of a single stage, cell recoveries measured 90–100% for average cell stream velocities ≥6 mm/s and for CVFs up to 20%. Cell recovery downstream of multistage devices also measured 90–100% after a critical device population time. This time was found to be five times the average cell residence time within the device. The measured recovery values were significantly larger than those typically obtained using conventional cell washing methods.

Keywords

Cryopreservation; Microfluidics; Biological cell; Cell processing; Laminar channel flow

1 Introduction

The use of microfluidics to manipulate populations of cells (as opposed to small numbers of individual cells) has been demonstrated in a number of studies. For example, Kumar and colleagues (2005) separated cells based on size using acoustic and flow fields. Sound waves

Correspondence to: Allison Hubel, hubel001@umn.edu.

were also employed by several investigators to move particles from one stream to another (Hawkes et al. 2004; Petersson et al. 2005). At very low cell concentrations (0.01% by volume), 70% of cells could be moved between the streams. A recent study by Di Carlo and colleagues (2007) used Dean vortices to focus a stream of particles (<1% by volume) into the center of a microfluidic channel. Yamada and colleagues (2008) used hydrodynamic filtration to exchange the carrier medium of cells rapidly in a suspension with very low cell volume fraction (CVF) (~0.02%).

Alternatively, Yang and colleagues (2005) employed the Zweifach-Fung effect in a microfluidic device to bleed off a percentage of blood plasma from an erythrocyte suspension. Although the hematocrit was significant (39%), the device features were extremely small, and the flow rate was 10 μL/h. Sethu and colleagues (2006a, b) used a microfluidic sieve to separate erythrocytes from leukocytes at flow rates of 5 μL/m.

Another application, which requires control of cell motion, involves the use of microfluidic devices for the introduction or removal of the specialized solutions used in cryopreservation. These solutions must be added to cell suspensions before freezing and removed when the suspensions are thawed. Centrifugation, the conventional method of removal, is labor intensive, time consuming, and inefficient in that 27–30% of the cells are lost during the removal process (Antonenas et al. 2002; Perotti et al. 2004) and in many situations, cells lost during processing cannot be replaced. In contrast to the applications described above, the suspension cytocrit for most cells being cryopreserved is much higher (2–20%). In addition, macroscopic suspension volumes (~30–500 ml) must be processed in relatively short times (less than 60 minutes). Once preserved cell suspensions are thawed prior to patient infusion, cell exposure to DMSO or other cryopreservatives must be minimized in order to avoid cell death (Fahy 1986). The studies described above demonstrate the potential of microfluidics as a platform for cell processing. However, none of these techniques on its own appears viable for the cryopreservation application. Specifically, these processes were designed to handle only small numbers of cells or cell suspensions with low concentrations. In addition, most of these studies did not require transport of chemical species (in this application, a cryopreservative solution) within the surrounding liquids.

In recent studies (Mata et al. 2008), we demonstrated removal of the cryopreservative DMSO from a 2% by volume cell suspension with a microfluidic device that allowed diffusion of DMSO from a cell suspension stream into a parallel wash stream. The cell recovery was greater than 90%. Separately, Glass et al. (2008) used a numerical model to determine appropriate geometries and operating conditions for removal of 95% of the DMSO (the reduction used in previous clinical studies) from a clinical scale volume of cell suspension (150 mL). The results suggested that an efficient device would require multiple serial washing stages to achieve this concentration reduction. The use of multiple stages in series enhances diffusion-based removal from the cell stream by increasing chemical gradients and transport in the cross stream direction.

The objective of the work described in this paper was to characterize the motion of cell suspensions through single and multi-stage two-stream devices. Below, we describe experiments in which cell-stream flow rate q_C and cell suspension cytocrit were varied. In

addition, we describe experiments designed to understand the transient portion of the suspension flow before steady flow rates are established. Our specific goals were to demonstrate effective cell recovery at clinical cytocrit levels and to determine the importance of transient effects on overall cell recovery from finite suspension volumes.

2 Methods

2.1 Flow device

A prototype with multiple serial channel stages (Fig. 1a) was fabricated and used to quantify cell viability and recovery. The key components of this prototype are the DMSO-removal devices, each of which includes a single rectangular channel (Fig. 1b, c). Each channel section is enclosed by two similar Lexan™ polycarbonate pieces machined with a computer numerical control mill that are held together with stainless steel screws and sealed with a custom-made Viton® O-ring. Constant cross-sectional area adapters are located at each end of the channel. A glass microscope cover slip (thickness = 170 μm) cut to size was mounted inside the adapter at the upstream end of the channel to act as a divider or splitter. Nylon fittings (not shown in Fig. 1b, c) are attached to the inlet and outlet ports, located on top and bottom sides of each adapter. Dimensions and a detailed description of the flow through the device follow.

Two streams enter the device through opposing ports(1.56 mm diameter) separated by the splitter plate. The splitter plate prevents mixing between the initially opposing streams and helps redirect the streams so that they flow in parallel. The upstream adapter, which has 25 mm length and a constant area cross-section of 12.5 mm^2, feeds both streams into the rectangular channel of d = 500 μm depth, 25 mm width, and 160 mm length (the splitter plate terminates at the downstream end of this adapter). Downstream of this section, a second constant area adapter is used to transition flow from the channel to the round outlet ports (1.56 mm diameter). The length over which diffusion occurs, from the tip of the splitter to the outlet ports, is 196 mm, and the total streamwise distance between inlet and outlet ports (including both adapters and the channel) is L = 232 mm.

Samples of both streams are collected downstream of the third stage exit; the wash stream sample is collected inline in a Tygon® tube section with volumetric capacity of 5 mL, and the cell-laden stream sample is collected in a vial.

2.2 Fluids

Phosphate-buffered saline solution (PBS) was used for the wash stream. The cell stream contained lymphoblasts (Jurkat cells, ATCC TIB-1522) suspended in a solution consisting of PBS with DMSO at 10% v/v to mimic a hematopoietic stem cell product. For all practical purposes, density and viscosity values for both solutions are approximated to ρ = 1 g/mL and μ = 1 cP (water properties), respectively.

The DMSO solution was introduced to the cell suspension using conventional methods. Briefly, cells were centrifuged, and the culture medium was aspirated and replaced with the DMSO solution. The volume of DMSO solution was adjusted to control both the cytocrit (concentration of cells 2–20%) and the final DMSO concentration (10% v/v). As exposure to

DMSO at room temperature can result in cell death, total time of exposure for the cells to DMSO was monitored and averaged 30–40 min.

2.3 Flow rate control and measurement

A syringe pump (Harvard Apparatus, Inc. Model 22) drives the cell-laden and wash solutions contained in two separate syringes simultaneously into the first stage (Fig. 1a). A small plastic Monoject syringe (20.40 mm cross-section diameter) drives the cell suspension, and a large plastic Monoject syringe (38.40 mm cross-section diameter) drives the wash stream. The volume of cell suspension V_0 was 20 mL, and the volume of wash solution in a given syringe was 140 mL. The desired flow rate (±0.1 mL/min) for the wash solution is set in a controller attached to the pump; this makes the piston driving the syringes move at a constant speed. The volumetric ratio at which both solutions are driven is then equal to the ratio of the cross-sectional area of the small and large syringes. To ensure that the volumetric ratio at which cell-laden and wash streams are separated at the outlet ports is the same ratio at which they entered the stage, a third syringe draws the wash stream leaving the stage at the same rate this solution is driven in. This is accomplished by attaching the third syringe to the back of the piston driving the other two syringes. Also, the cross-sectional area of the syringes driving and drawing the wash stream must be the same. The cell-laden stream outlet is connected to the cell-laden stream inlet port of the second stage. Another pair of syringes, also attached to the syringe pump, drives/draws the wash stream through the second stage. This scheme repeats itself for the third and last stage, except for the cell-laden stream outlet port, which is open to the atmosphere. Tubing connecting syringes and channels had inner diameter of 0.8 mm. The tube between the cell suspension syringe and the first channel had a length of 457 mm, and cell-stream tubing between channel pairs and downstream of the final stage outlet port had lengths of 64 mm.

2.4 Stream characterization

2.4.1 Cell viability and cell recovery—

Cell recovery from the device was determined using a hematocytometer (Hausser Scientific) combined with a membrane integrity dye. A sample of cell suspension was recovered from the device outlet and stained for membrane integrity using acridine orange and propidium iodine. Cells that fluoresce green have intact membranes and are considered live, while those that fluoresce orange are considered dead. Viability is defined as the number of cells that fluoresce green divided by the total number of fluorescing cells. Viable cell recovery is defined as the number of viable cells flowing out of the device divided by the number of viable cells flowing into the device:

$$\text{Recovery} = \frac{\text{Viability}_{\text{out}} \times \text{CVF}_{\text{out}}}{\text{Viability}_{\text{in}} \times \text{CVF}_{\text{in}}}, \quad (1)$$

where CVF_{out} denotes the CVF at the cell-stream outlet and CVF_{in} the CVF at the cell-stream inlet. There are two basic mechanisms of cell losses in the device: (1) the cell is intact but has lost viability and (2) the cell has lysed or become trapped in the device. Quantifying viable cell recovery permits us to quantify cell losses from both of those mechanisms. Because cell counts performed with a hematocytometer can vary over a range

of ~20% even with a skilled operator, the uncertainty in individual viability and recovery measurements is fairly high.

Our previous studies (Mata et al. 2008) suggested that a start-up period is required for cells to populate the device before a steady state outflow of cells occurs. Thus, cell viability and recovery tests were carried out both during this start-up period and after steady state was achieved. Cell-laden stream samples (1.6 mL) were collected after 20, 40, 60, and 80% of the cell suspension had been displaced by the driving syringe.

In this paper, the dimensionless displaced (or processed) volume is denoted by

$$V^* = \frac{V}{V_0} \quad (2)$$

where V_0 is initial volume of cell suspension inside the driving syringe and V is the displaced volume at any time. If the cell-stream flow rate q_C is constant, the time needed to displace V, is

$$t = \frac{V}{q_C}. \quad (3)$$

If q_C is constant but the number of stages is increased, the actual (dimensional) residence time of a given cell within the device increases also. In addition, if the number of stages is constant but q_C is decreased, the residence time increases.

The residence time can thus be defined as

$$t_{RES} = \frac{L_C}{\bar{u}_C} + \frac{L_{tube}}{\frac{A_{tube}}{A_C}\bar{u}_C} = \frac{L_C}{\bar{u}_C}\left(1 + \frac{L_{tube}A_C}{L_C A_{tube}}\right), \quad (4)$$

where A_C is the cell stream cross-sectional area, $\bar{u}_C = \frac{q_C}{A_C}$ the average cell stream velocity, L_C is the total distance travelled by the cells inside the channel sections, i.e. the length between input and output ports multiplied by the number of stages, L_{tube} is the distance travelled through tubes between stages, and A_{tube} is the tube cross-sectional area. Notice that L_C doubles if two stages are used instead of one and triples if three stages are used. Here, $A_C = w\delta$, where w is the channel width or span, and δ is the depth of the cell stream. The Reynolds number based on the average velocity and depth of the cell stream is defined as $Re = \frac{\rho \bar{u}_C \delta}{\mu}$.

In the channel section, the depth ratio δ/d is directly related to the inlet flow rate fraction $f_q = \frac{q_C}{q_T}$; where q_T is the total volumetric flow rate through the channel such that $q_T = q_C + q_W$, and q_W is the wash stream flow rate. The flow rate fraction f_q is related to δ/d through the parabolic velocity profile across the channel depth. In the above definition, we neglect the residence time of cells in tubing before the first channel stage (This tube is primed with cell suspension before starting the experiment at $t = 0$). The residence time in each of the tubes between neighboring stages and downstream of the final stage outlet port is 3.5% of the time within a single stage. These individual factors will be discussed in Sect. 3 below.

The dimensionless time t^* needed to displace V^* can be defined as

$$t^* = \frac{t}{t_{RES}} = t\left(\frac{\bar{u}_C}{L_C}\right)/\left(1 + \frac{L_{tube}A_C}{L_C A_{tube}}\right). \quad (5)$$

Note that $t^* = 1$ is the average dimensionless time required for a cell to travel from the inlet port to the outlet port.

By combining Eqs. 2–5, the following relationship between t^* and V^* is found:

$$t^* = V^*\left(\frac{V_0}{A_C L_C}\right)/\left(1 + \frac{L_{tube}A_C}{L_C A_{tube}}\right). \quad (6)$$

The effect of number of stages (one, two and three), the cell-laden stream flow rate q_C (0.87, 1.41, and 1.98 mL/min), and the volume fraction of the cell suspension CVF (2, 8, and 20%) was studied for $f_q = 0.23$. Seven parametric conditions were tested. For each condition, three independent counts were performed per displaced volume V^* (including $V^* = 0$, at the inlet) for a total of 105 counts: 21 at the inlet and 84 at the outlet. Mean values of viability, cell concentration, and recovery were calculated. The results are expressed as the mean ± SD (standard deviation).

3 Results

3.1 Cell recovery from a single stage device

The motion of cells through the microfluidic channel is influenced by the flow rate of the cell-laden stream q_C, and the CVF. In order to quantify transient effects, cell recovery from a single stage device was measured as a function of flow conditions after various processing times. Cell counts were performed at the inlet and outlet of the device to quantify cell recovery for $q_C = 0.85$, 1.41, and1.98 mL/min ($\bar{u}_C = 3.6$, 6.0, and 8.5 mm/s) with CVF held constant, as well as for CVF = 2, 8, and 20% (with q_C held constant). Cell counts were performed on samples from both the wash and cell-laden streams. In this paper, only the latter are reported, since the concentration of cells in the wash stream was always below the level of detection for the hematocytometer implying that any migration of cells into the wash

stream was minimal. Resulting measurements of cell viability, recovery, and CVF_{out}/CVF_{in} in the cell-laden stream are listed in Tables 1–3.

The viability at the inlet was close to 0.90. For most flow conditions, the viability measured at the outlet was slightly higher than the viability at the inlet, i.e. a smaller percentage of dead cells was counted at the outlet (Tables 1–3). DMSO has been shown to permeabilize cells (Gurtovenko and Anwar 2007). The lower fraction of cells staining as intact at the inlet of the device may reflect not a lower viability but rather a higher degree of permeation for membrane dyes normally excluded from the cells when viable because of the permeabilizing affect of DMSO.

3.1.1 Effect of cell-stream flow rate (q_C)—Samples of the cell-laden stream were collected at the inlet and outlet of a single stage device at different times t^*. Resulting measurements of cell viability, recovery, and CVF_{out}/CVF_{in} for $f_q = 0.23$ and CVF = 2% are shown in Table 1. Cell recovery values for the same flow conditions are also plotted in Fig. 2. Cell recoveries were larger for the two higher flow rates $q_C = 1.41$ and 1.98 mL/min ($\bar{u}_C$ = 6 and 8.5 mm/s). Although there is scatter associated with uncertainty in the results, all of the values are of order 90–100%. As noted previously, no cells were observed in the wash stream. Cell recovery for the lowest flow rate $q_C = 0.85$ mL/min ($\bar{u}_C = 3.6$ mm/s) was noticeably lower at all measurement times t^*. Thus, the three cases do not collapse according to the dimensionless residence time (Fig. 2). Further, the lowest cell-stream flow rate ($q_C = 0.85$ mL/min) yields variations in cell recovery (and the ratio CVF_{out}/CVF_{in}) with t^*. The recovery value starts low (0.73), reaches a maximum (0.88), and then decreases again to 0.73 (Table 1, Fig. 2).

A possible explanation for the early increase in recovery with time is that, at this flow rate, it takes a longer time (t^*) to 'populate' the channel before a steady flow rate of cells is observed (and counted) at the outlet. In previous cell motion studies, Mata et al. (2008) obtained top view images of Jurkat cells in a DMSO solution flowing through a single stage channel for $q_C = 0.28$, 0.85, and 1.41 mL/min, $f_q = 0.23$ and CVF = 2%. It was observed that cells tend to pack more tightly for lower cell stream flow rates. These observations, combined with the present results, suggest that steady state conditions are achieved only after a critical cell packing (or critical cell 'hold up') is reached. At this time ($t^*_{critical}$), the device is fully populated, and the measured recovery reaches a maximum. In other words, only after $t^*_{critical}$ does the rate of cell outflow equal the rate of inflow. Furthermore, the slower the flow, the longer it takes to reach the critical 'hold up', and the larger the value of the critical 'hold up'. To quantify these trends further, additional experiments would be required in which the critical hold up is measured as a function of q_C and other flow conditions.

We believe that the decrease in cell recovery for $q_C = 0.85$ mL/min when $t^* = 17.8$ ($V^* = 0.8$) shown in Fig. 2 is probably caused by changes in the inlet CVF. We have presumed, thus far, that the inlet CVF is constant throughout a given test run. Separate experiments were performed to quantify the variations in inlet CVF with time. Suspensions of Jurkat cells in 10% DMSO with average $CVF_0 = 0.02$ (CVF = 2%) were driven horizontally from a

20 mL syringe using a range of flow rates (q_C = 0.85, 1.4, and 2.0 mL/min) and collected immediately downstream of the syringe tip. Figure 3 shows the normalized CVF* = CVF_{tip}/CVF_0 as a function of V^*, parameterized by the flow rate q_C. During the initial portion of the run, CVF* remained nearly constant. For longer processing times (and larger V^*), cells settled in the syringe and CVF* decreased. Changes in the inlet CVF flowing into the device can also influence the outflow of cells by changing the apparent CVF.

3.1.2 Effect of CVF—Measurements of cell viability, recovery, and CVF_{out}/CVF_{in} for tests with f_q = 0.23, q_C = 1.41 mL/min, and CVF = 2, 8 and 20% are shown in Table 2. Cell recovery values for the same flow conditions are also plotted in Fig. 4. As stated earlier, cell viabilities were high at the outlet (~0.90) for all three volume fractions. The CVF = 2% case (Table 1) yielded high recovery values at all measurement times. The recovery is also high for CVF = 8 and 20% (~0.9 or larger) although the values drop to 0.85 when t^* = 17.8 (V^* = 0.80). The ratio CVF_{out}/CVF_{in} given in Table 2 reveals a similar trend. The high recovery results at t^* = 4.4 (V^* = 0.2) suggest that, for these flow conditions (q_C = 1.41 mL/min, f_q = 0.23, and CVF up to 20%), a t^*critical has probably been reached. The small decrease in recovery for CVF = 8 and 20% at t^* = 17.8 (Table 2, Fig. 4), however, is again likely related to cell settling and accumulation within the driving syringe. As occurred for low cell stream flow rate (Fig. 3, q_C = 0.85 mL/min), a significant volume fraction of cells (larger than the measured CVF_{in}) remained inside the driving syringe when the experiment was stopped at V^* = 0.8. In future experiments, we believe that this problem could be mitigated by reorienting the driving syringes into a vertical position. This way, the settling cells would be driven into the device, guaranteeing high cell recovery because few to no cells would remain in the syringe at the end of the experiment. In any case, the location and orientation of suspension reservoirs is likely to affect instantaneous and possibly overall recoveries in applications requiring processing of significant volumes of cell suspension.

3.2 Cell recovery from a multi-stage device

To further investigate the effect of the residence time, samples of the cell-laden stream were collected at the inlet and outlet of one, two, and three-stage devices at different times t^*. The flow conditions were f_q = 0.23, q_C = 1.41 mL/min and CVF = 2%. The results of these tests, including, viability, recovery, and CVF_{out}/CVF_{in} are given in Table 3, and the recovery values are plotted in Fig. 5.

In general, the viability at the outlet was slightly higher than the viability at the inlet as before, meaning again that fewer dead cells were counted at the outlet. Therefore, processing times of up to 10 min resulted in no significant cell death by exposure to DMSO. This is not surprising since due to the nature of the device, DMSO levels within the cell suspension are reduced very quickly in the first channel stage to a fraction of the original level (Fleming et al. 2007). An exception occurred for the three-stage configuration at V^* = 0.2 (t^* = 1.5, the smallest dimensionless time captured). At this early time, the viability at the device outlet was lower (0.59) than at the inlet (0.91). We are unsure of the cause of this anomalous result. As the viability of cells at the outlet increased strongly for later V^* and t^*, it is unlikely that the reduced viability observed at V^* = 0.2 reflects cell death resulting from the cell stream flowing through three stages.

The most important point to notice from Table 3 is that cell recoveries from the three-stage device are low in general, but they increase with t^*. This behavior is explained clearly by the plot in Fig. 5. Because the distance travelled by the cells L_C is large for the three-stage device, the values of t^* obtained are small, and importantly below $t^*_{critical}$. Higher values of t^* could not be reached for this configuration because of the limited syringe volume available for the cell suspension. Note also in Fig. 5 that data from the three configurations collapse nicely in terms of t^*. Recovery from the single stage device was high (~100%) for all t^*, and similar recovery was obtained from the two-stage device at later times. Based on the collective data at these flow conditions, it appears that $t^*_{critical} \sim 5$, meaning that a period of $5t_{RES}$, where t_{RES} is the average passage time, is needed to fully populate the channel. The data in Fig. 5 were plotted separately using a t_{RES} that included only the passage time through the channel sections (Eq. 5). The resulting plot, which was nearly indistinguishable from the one presented herein, demonstrated that cell residence time in the tubes connecting multiple stages was effectively negligible compared with residence time in the channel sections.

4 Discussion

The long population time required for the three-stage device can be explained by the strong variation in streamwise velocity across the cell suspension flow stream. Here, we assume that cells travel with the local fluid velocity. Although the average velocity in the cell stream, $\bar{u}_C$ in the expression for t_{RES}, is about 6 mm/s for the test condition q_C = 1.4 mL/min, the local velocity actually ranges from 10.4 mm/s down to zero at the wall. Therefore, a volume of cell suspension introduced into the two-stream channel experiences very strong streamwise dispersion across the cell stream. Cells travelling closer to the channel centerplane move rapidly, but cells travelling close to the wall move much more slowly and therefore, in the absence of gravity, the population time for heights just above the channel wall is very long. For example, under these conditions, the velocity 10 lm above the wall is less than 1 mm/s. Thus, the result that the critical t^* for populating the device is of order 5, rather than one, suggests that the slow flow close to the channel wall plays a significant role.

For our goal of processing clinical samples of relatively large volume (150 mL), any loss associated with population of the channels would be a small fraction of the total number of cells processed. In practice, one would begin capturing cells at the device outlet after a time of approximately t_{RES} and perhaps complete capture after an additional time $T^* = V_0/(A_cL_c)$ beyond which all of the original cell suspension has been driven into the system (the flow could be run for additional time by post-priming the inlets). For the example considered in Glass et al. (2008) of a 150 mL sample of suspension requiring processing in 60 min, the current three-stage set up could be scaled up in width (new width = 1.8 × 25 mm) to achieve the required flow rate as well as the required level of DMSO extraction. In this case, the volume of cell suspension within the three-stage system would be 4.8 mL, and T^* = 31.3. If we then estimate the percentage of cells recovered from t_{RES} to $t_{RES} + T^*$ using a crude fit to the data in Fig. 4 and assume no losses other than those associated with populating the system, we obtain 92%. If the capture time is extended further, the percentage of cells captured would obviously rise. Therefore, the issue of populating the system does not appear

to be a significant problem for processing relatively large sample volumes, especially compared against the lower recoveries achieved by centrifugation methods (~70–73%; Antonenas et al. 2002; Perotti et al. 2004). For small sample volumes, the presence of strong streamwise dispersion within an extraction device could become a significant issue, however, as capture times for small volumes would have to be relatively large leading to significant dilution of the original suspension.

5 Conclusions

The experiments described in this paper demonstrated two important points relevant to processing significant volumes of cell suspensions with high cytocrits in relatively short periods of time.

First, cell recovery was 90–100% for average cell stream velocity equal to or above 6 mm/s ($Re \geq 4.3$) for CVFs up to 20%. The measured recovery values were significantly larger than those typically obtained using conventional cell washing methods. The results imply that cells are not damaged within the flow device, and that they remain confined within the depth of their original flow stream so that they are easily recaptured at the device outlet.

Second, a two-stream channel device requires a population time before reaching steady state, and this time can be estimated based on the average cell passage time through the device. Tubing between channel stages has only a minimal effect on this time because velocities through the tubing are typically much higher than velocities in channel sections. For the flow rate fraction of 23% considered herein, this population time was estimated as $5t_{RES}$. Recoveries of less than 90% measured in multistage configurations were caused not by losses but rather by the requirement to populate the channels with cells and reach a true steady state.

Acknowledgments

This work was funded by the National Institutes of Health (R21EB004857). The authors thank Dave Hultman for assistance with facility design, Brian Darr for help with cell culturing and Jacob Hanna for help with additional experiments.

References

Antonenas V, Bradstock K, Shaw P (2002) Effect of washing procedures on unrelated cord blood units for transplantation in children and adults. Cytotherapy 4:16

Di Carlo D, Irimia D, Tompkins RG, Toner M (2007) Continuous inertial focusing, ordering, and separation of particles in microchannels. Proc Natl Acad Sci USA 104:18892–18897 [PubMed: 18025477]

Fahy GM (1986) The relevance of cryoprotectant “toxicity” to cryobiology. Cryobiology 23(1):1–13 [PubMed: 3956226]

Fleming KK, Longmire EK, Hubel A (2007) Numerical characterization of diffusion-based extraction in cell-laden flow through a microfluidic channel. J Biomech Eng 129:703–711 [PubMed: 17887896]

Glass K, Longmire EK, Hubel A (2008) Optimization of a micro-fluidic device for diffusion-based extraction of DMSO from a cell suspension. Int J Heat Mass Transfer 51(23):5749–5757

Gurtovenko AA, Anwar J (2007) Modulating the structure and properties of cell membranes: the molecular mechanism of action of dimethyl sulfoxide. J Phys Chem B 111:10453–10460 [PubMed: 17661513]

Hawkes JJ, Barber RW, Emerson DR, Coakley WT (2004) Continuous cell washing and mixing driven by an ultrasound standing wave within a microfluidic channel. Lab Chip 4:446–452 [PubMed: 15472728]

Kumar M, Felke D, Belovick J (2005) Fractionation of cell mixtures using acoustic and laminar flow fields. Biotechnol Bioeng 89:129–137 [PubMed: 15593262]

Mata C, Longmire E, McKenna D, Glass K, Hubel A (2008) Experimental study of diffusion based extraction from a cell suspension. Microfluid Nanofluid 5:529–540

Perotti CG, Fante CD, Viarengo G, Papa P, Rocchi L, Bergamaschi P, Bellotti L, Marchesi A, Salvaneschi L (2004) A new automated cell washer device for thawed cord blood units. Transfusion 44:900–906 [PubMed: 15157258]

Petersson F, Nilsson A, Jonsson H, Laurell T (2005) Carrier medium exchange through ultrasonic particle switching in microfluidic channels. Anal Chem 77:1216–1221 [PubMed: 15732899]

Sethu P, Moldawer LL, Mindrinos MN, Scumpia PO, Tannahill CL, Wilhelmy J, Efron PA, Brownstein BH, Tompkins RG, Toner M (2006a) Microfluidic isolation of leukocytes from whole blood for phenotype and gene expression analysis. Anal Chem 78:5453–5461 [PubMed: 16878882]

Sethu P, Sin A, Toner M (2006b) Microfluidic diffusive filter for apheresis (leukapheresis). Lab Chip 6:83–89 [PubMed: 16372073]

Yamada M, Kobayashi J, Yamato M, Seki M, Okano T (2008) Millisecond treatment of cells using microfluidic devices via two-step carrier-medium exchange. Lab Chip 8:772–778 [PubMed: 18432348]

Yang S, Undar A, Zahn JD (2005) Blood plasma separation in microfluidic channels using flow rate control. ASAIO J 51:585–590 [PubMed: 16322722]

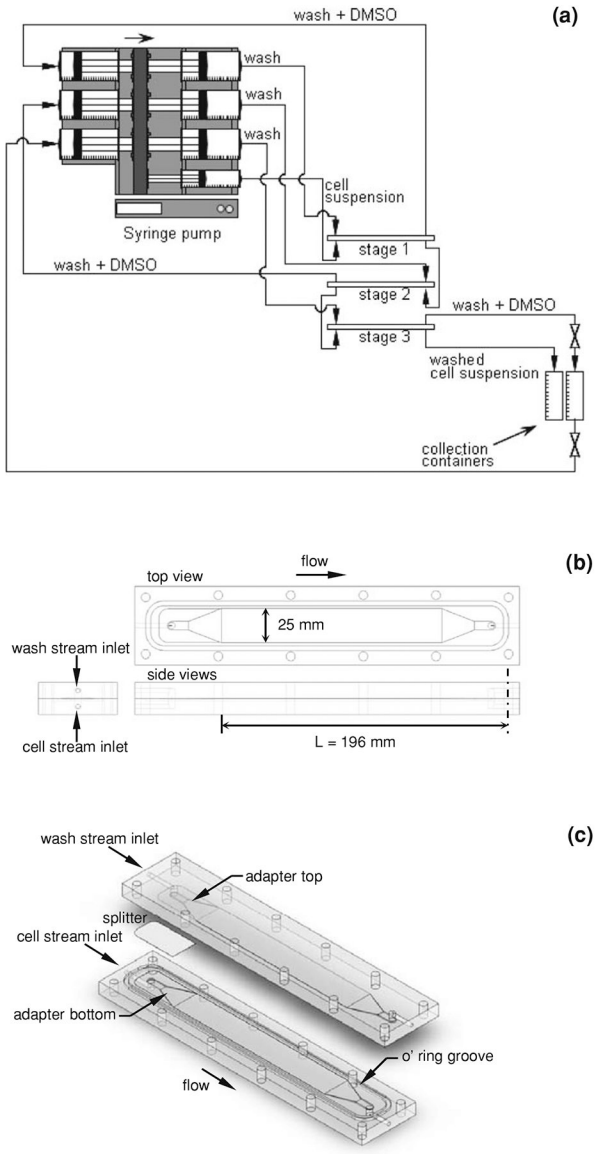

Fig. 1.

a Sketch of experimental set up. The cell suspension is driven into stage 1 by a small syringe. Fresh wash is driven into each stage by three independent large syringes. Wash + DMSO is drawn from each stage by three independent large syringes.**b** Sketch of one stage (to scale), and **c** exploded view of the stage (to scale)

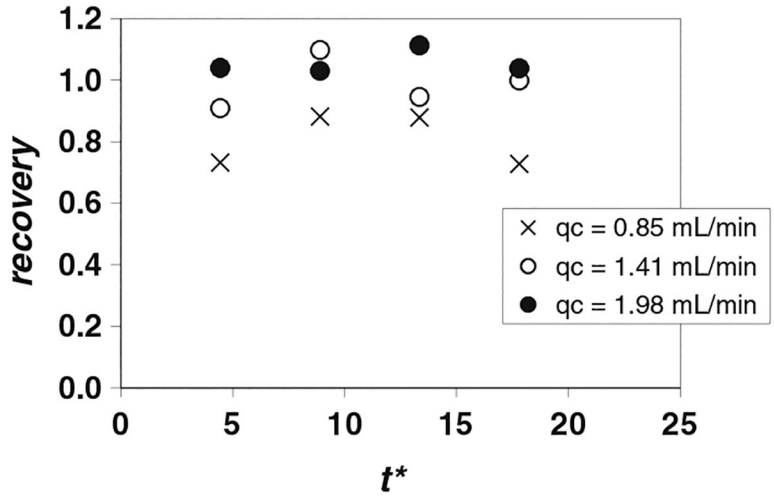

Fig. 2.

Cell recovery as a function of dimensionless time t^* for $f_q = 0.23$ and CVF = 2%, parameterized by the cell-laden stream flow rate q_C ($Re = 2.6–6.0$) for a single stage device. Suspension of Jurkat cells in 10% DMSO

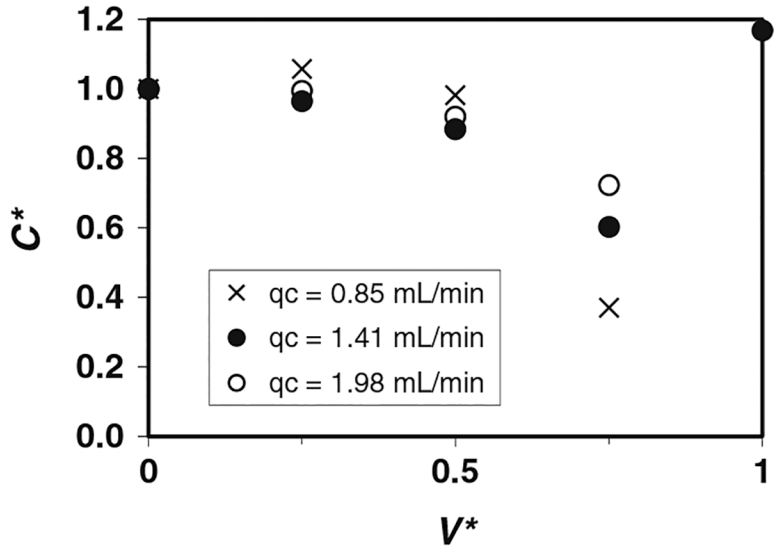

Fig. 3.

Normalized cell volume fraction CVF* = CVF_{tip}/CVF_0 at the outlet of a 20 mL syringe as a function of displaced volume V^*, parameterized by the flow rate q_C (Re = 2.6–6.0). Suspension of Jurkat cells in 10% DMSO with average cell concentration CVF_0 = 2%

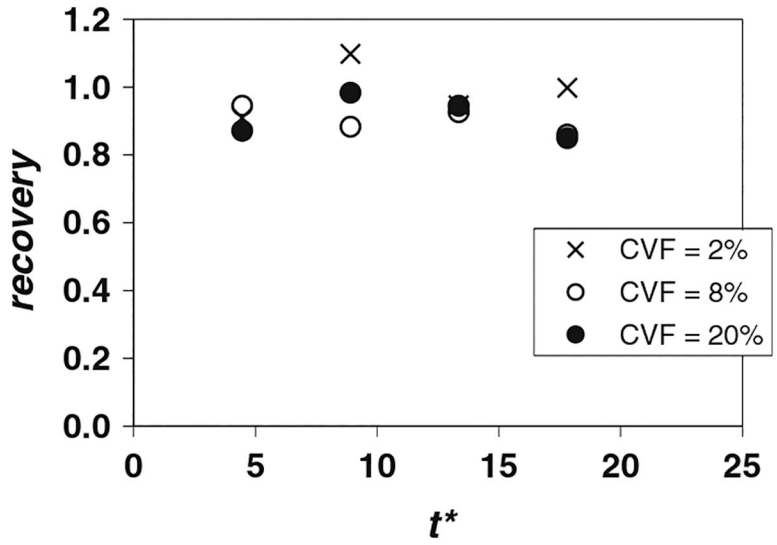

Fig. 4.

Cell recovery as a function of dimensionless time t^* for $f_q = 0.23$ and $q_C = 1.41$ mL/min ($Re = 4.3$), parameterized by the cell volume fraction (CVF). Suspension of Jurkat cells in 10% DMSO

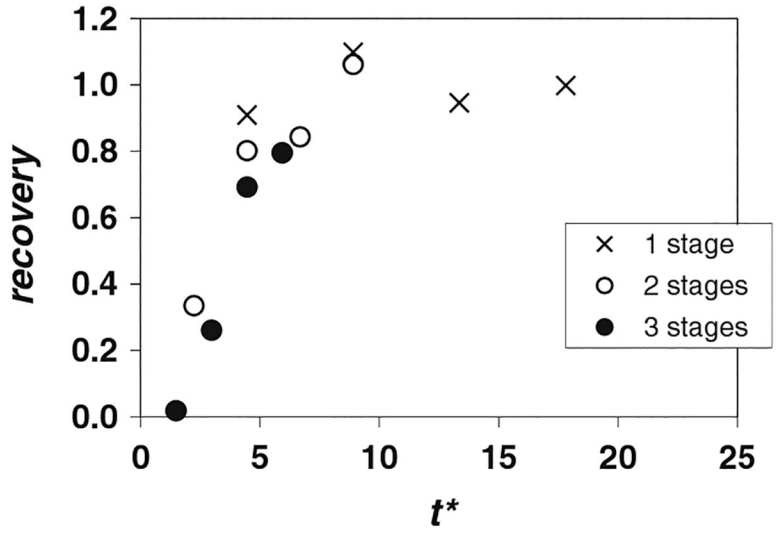

Fig. 5.

Cell recovery as a function of dimensionless time t^* for $f_q = 0.23$ and $q_C = 1.41$ mL/min ($Re = 4.3$). Suspension of Jurkat cells in 10% DMSO with CVF = 2%. Multi-stage device

Table 1

Recovery of Jurkat cells in 10% DMSO suspension from a single stage device with CVF = 2% and f_q = 0.23. Results are reported as mean ± SD

Re	q_C **(mL/min)**	**Cell suspension processed volume (*V**)**	**Viability$_{in}$**	**Viability$_{out}$**	**Recovery**	**CVF$_{out}$/CVF$_{in}$**
2.6	0.85	0.2	0.90 ± 0.02	0.93 ± 0.03	0.73 ± 0.10	0.70 ± 0.07
		0.4		0.95 ± 0.02	0.88 ± 0.17	0.83 ± 0.15
		0.6		0.93 ± 0.02	0.88 ± 0.06	0.85 ± 0.05
		0.8		0.94 ± 0.02	0.73 ± 0.04	0.69 ± 0.03
4.3	1.41	0.2	0.87 ± 0.04	0.89 ± 0.04	0.91 ± 0.09	0.89 ± 0.07
		0.4		0.91 ± 0.02	1.10 ± 0.02	1.04 ± 0.02
		0.6		0.90 ± 0.02	0.95 ± 0.06	0.91 ± 0.04
		0.8		0.92 ± 0.02	1.00 ± 0.08	0.94 ± 0.04
6.0	1.98	0.2	0.89 ± 0.02	0.93 ± 0.03	1.04 ± 0.17	1.00 ± 0.16
		0.4		0.93 ± 0.02	1.03 ± 0.13	0.99 ±0.11
		0.6		0.92 ± 0.02	1.11 ± 0.14	1.08 ± 0.13
		0.8		0.94 ± 0.02	1.04 ± 0.15	0.99 ± 0.15

Table 2

Recovery of Jurkat cells in 10% DMSO suspension from a single stage device for $f_q = 0.23$, $q_C = 1.41$ mL/min and $Re = 4.3$. Results are reported as mean ± SD

CVF (%)	Cell suspension processed volume (V^*)	$Viability_{in}$	$Viability_{out}$	Recovery	CVF_{out}/CVF_{in}
2	0.2	0.87 ± 0.04	0.89 ± 0.04	0.91 ± 0.09	0.89 ± 0.07
	0.4		0.91 ± 0.02	1.10 ± 0.02	1.04 ± 0.02
	0.6		0.90 ± 0.02	0.95 ± 0.06	0.91 ± 0.04
	0.8		0.92 ± 0.02	1.00 ± 0.08	0.94 ± 0.04
8	0.2	0.90 ± 0.02	0.92 ± 0.02	0.95 ± 0.04	0.92 ± 0.02
	0.4		0.93 ± 0.02	0.88 ± 0.09	0.86 ± 0.10
	0.6		0.93 ± 0.02	0.93 ± 0.06	0.90 ± 0.07
	0.8		0.92 ± 0.02	0.86 ± 0.02	0.84 ± 0.01
20	0.2	0.89 ± 0.01	0.91 ± 0.03	0.87 ± 0.07	0.84 ± 0.06
	0.4		0.93 ± 0.02	0.98 ± 0.07	0.93 ± 0.09
	0.6		0.91 ± 0.03	0.95 ± 0.04	1.08 ± 0.02
	0.8		0.91 ± 0.02	0.85 ± 0.02	0.82 ± 0.04

Table 3

Recovery of Jurkat cells in 10% DMSO suspension with CVF = 2% for f_q = 0.23, q_C = 1.41 mL/min and Re = 4.3. Results are reported as mean ± SD

No. of stages	Cell suspension processed volume (V^*)	$Viability_{in}$	$Viability_{out}$	Recovery	CVF_{out}/CVF_{in}
1	0.2	0.87 ± 0.04	0.89 ± 0.04	0.91 ± 0.09	0.89 ± 0.07
	0.4		0.91 ± 0.02	1.10 ± 0.02	1.04 ± 0.02
	0.6		0.90 ± 0.02	0.95 ± 0.06	0.91 ± 0.04
	0.8		0.92 ± 0.02	1.00 ± 0.08	0.94 ± 0.04
2	0.2	0.91 ± 0.02	0.85 ± 0.12	0.34 ± 0.15	0.34 ± 0.12
	0.4		0.93 ± 0.02	0.80 ± 0.02	0.77 ± 0.02
	0.6		0.95 ± 0.01	0.84 ± 0.04	0.79 ± 0.01
	0.8		0.96 ± 0.01	1.06 ± 0.14	0.99 ± 0.10
3	0.2	0.91 ± 0.03	0.59 ± 0.13	0.02 ± 0.02	0.03 ± 0.03
	0.4		0.86 ± 0.06	0.26 ± 0.05	0.28 ± 0.06
	0.6		0.95 ± 0.02	0.69 ± 0.03	0.67 ± 0.05
	0.8		0.95 ± 0.02	0.80 ± 0.03	0.76 ± 0.01